JCTC Journal of Chemical Theory and Computation

Calculation of Fukui Functions Without Differentiating to the Number of Electrons. 3. Local Fukui Function and Dual Descriptor

Tim Fievez,[†] Nick Sablon,[†] Frank De Proft,[†] Paul W. Ayers,[‡] and Paul Geerlings*,[†]

Eenheid Algemene Chemie (ALGC), Vrije Universiteit Brussel (VUB), Pleinlaan 2, 1050 Brussel, Belgium, and Department of Chemistry, McMaster University, Hamilton, Ontario L8S 4M1, Canada

Received January 25, 2008

Abstract: An alternative approach for the calculation of DFT-based reactivity descriptors involving derivatives of the energy with respect to the number of electrons and the external potential is further evaluated. Using functional derivatives with respect to the external potential, the finite difference approximation was avoided for the local calculation of the Fukui functions and the dual descriptor. A relevant set of molecules has been calculated after the optimization of computational parameters. It is shown that the new approach correctly predicts the nucleophilic attack on CH_2O, the formation of CO metal complexes, the regioselectivity of monosubstituted benzenes, and the softest nucleophilic site in some ambident nucleophiles.

1. Introduction

Density functional theory (DFT), with the electron density ($\rho(\bar{r})$) as the central quantity, provides an extraordinary tool for the theoretical study of chemical systems. On the basis of the Hohenberg and Kohn theorems[1] and the subsequent work of Kohn and Sham,[2] DFT[3,4] became highly popular as an ab initio method during the past two decades, mainly due to the development of accurate exchange-correlation functionals[5,6] and the implementation of the formalism in mainstream ab initio programs.

The advantages of DFT mainly focus on its superior accuracy per unit computational cost and the possibility of defining chemical concepts in a precise way using the so-called conceptual DFT.[7–10] This flourishing DFT domain, founded by Parr and co-workers, creates a theoretical framework for various chemical reactivity concepts, allowing their qualitative and quantitative use in reactivity studies. For example, quantities such as electronegativity,[11] hardness,[12] and softness[13] received a strict definition in DFT. Insight into the different descriptors showed that most reactivity descriptors are defined as derivatives of the electronic energy with respect to the number of electrons or the external potential.[14] (For an isolated system, the external potential is the potential caused by the atomic nuclei.) The Fukui function $f(\bar{r})$,[15] for example, is defined as the (mixed) variational derivative of the energy with respect to the number of electrons N and the external potential $v(\bar{r})$:

$$f(\bar{r}) = \frac{\partial^2 E}{\partial N \delta\, v(\bar{r})} \tag{1}$$

A simpler form of the Fukui function can be formulated using the electron density, $\rho(\bar{r})$:

$$f(\bar{r}) = \left(\frac{\partial\, \rho(\bar{r})}{\partial N}\right)_{v(\bar{r})} \tag{2}$$

Formulas 1 and 2 are problematic since the "derivative discontinuity" in the energy (and the density) with respect to the number of electrons[16–21] makes $f(\bar{r})$ undefined for an integer number of electrons and hence for any isolated molecule. This can be overcome by introducing derivatives from the right, f^+, and from the left, f^-. In line with Perdew et al.'s[16,17] conclusions, these derivatives can be computed exactly with the electron densities of the anionic ($\rho_{N+1}(\bar{r})$), cationic ($\rho_{N-1}(\bar{r})$), and neutral systems ($\rho_N(\bar{r})$):[19,21]

$$f_N^+(\bar{r}) = \left(\frac{\partial\, \rho_N(\bar{r})}{\partial N}\right)^+_{v(\bar{r})} = \rho_{N+1}(\bar{r}) - \rho_N(\bar{r}) \tag{3}$$

$$f_N^-(\bar{r}) = \left(\frac{\partial\, \rho_N(\bar{r})}{\partial N}\right)^-_{v(\bar{r})} = \rho_N(\bar{r}) - \rho_{N-1}(\bar{r}) \tag{4}$$

* Corresponding author e-mail: pgeerlin@vub.ac.be.
[†] Vrije Universiteit Brussel.
[‡] McMaster University.

10.1021/ct800027e CCC: $40.75
Published on Web 05/27/2008

The Fukui function from above, f^+, represents the best way to change the electron density in response to an increase in the number of electrons; consequently, it can be employed to predict the preferred site for a nucleophilic attack. The Fukui function from below, f^-, represents the best way to change the electron density in response to a decrease in the number of electrons; consequently, it can be employed to predict the preferred site for an electrophilic attack.

Since practical DFT calculations generally use approximate exchange-correlation functionals with a N-electron self-interaction error,[22] eqs 3 and 4 are not exact anymore. Although the finite difference expressions are only approximate[19,20,23,24] for those situations, they are conventionally used as the reference method for the calculation of Fukui functions. This is justified by the fact that approximate exchange-correlation functionals are usually more accurate for systems with integer numbers of electrons than they are for systems with fractional electron numbers. For example, the ionization potentials computed by the finite difference approximation are more accurate than those computed from the highest occupied molecular orbital (HOMO) energy.[25]

Examination of the higher-order energy derivatives can lead to new descriptors of chemical importance.[26] Morell et al. introduced the dual descriptor[27–30] this way:

$$f^{(2)}(\bar{r}) = \frac{\partial^3 E}{\partial^2 N \delta\, v(\bar{r})} \tag{5}$$

The actual significance of this new descriptor becomes clear by incorporating the definition of the Fukui function:

$$f^{(2)}(\bar{r}) = \left(\frac{\partial f(\bar{r})}{\partial N}\right)_{v(\bar{r})} \cong f^+(\bar{r}) - f^-(\bar{r}) \tag{6}$$

Within this finite difference approximation, the dual descriptor can be interpreted as the difference between the Fukui functions for nucleophilic and electrophilic attacks. The dual descriptor thus gives a combination of both Fukui functions: it is positive for locations where a nucleophilic attack is more probable than an electrophilic attack and negative where electrophilic attack is more probable.

The theoretical basis for the dual descriptor is explained in ref 28, as is its application to various molecules. Its usefulness has been shown by the determination of the regioselectivities in the electrophilic aromatic substitutions on monosubstituted benzenes[27] and other organic reaction types.[29–31]

In this article, a recent approach for the calculation of Fukui functions, presented by some of the authors,[32,33] is further evaluated and extended for the dual descriptor. The Fukui function is calculated as the functional derivative of the electronic chemical potential to the external potential:

$$f(\bar{r}) = \left(\frac{\delta \mu}{\delta\, v(\bar{r})}\right)_N \tag{7}$$

This alternative definition can easily be obtained from eq 2 using a Maxwell relation. The derivative can then be calculated on the basis of the responses of the electronic chemical potential (μ) to a large number of perturbations in the external potential modeled by randomly placed point charges.

As the dual descriptor can be expressed in terms of the functional derivative of the hardness to the external potential, an analogous scheme can be developed for its calculation.

2. Methodology

2.1. Functional Derivatives. When the derivative discontinuity is taken into account, the following definitions for the Fukui functions can be rewritten as

$$f_N^+ = \left(\frac{\delta \mu_N^+}{\delta\, v(\bar{r})}\right)_N \tag{8}$$

$$f_N^- = \left(\frac{\delta \mu_N^-}{\delta\, v(\bar{r})}\right)_N \tag{9}$$

Similar to formulas 3 and 4, the finite difference approximation seems inevitable for the evaluation of μ^+ and μ^- if an approximate exchange-correlation functional is used. In this case, the proposed formulas 8 and 9 would give the same result as eqs 3 and 4. However, because the exchange-correlation potentials associated with the local density approximation (LDA) and generalized gradient approximations (GGAs)[34,35] do not have a "derivative discontinuity", the orbital energies are exactly equal to the chemical potentials in those approximations.[36–38]

$$\mu^+ = \varepsilon_{\mathrm{LUMO}} \tag{10}$$

$$\mu^- = \varepsilon_{\mathrm{HOMO}} \tag{11}$$

Here, $\varepsilon_{\mathrm{LUMO}}$ denotes the lowest unoccupied molecular orbital (LUMO) energy and $\varepsilon_{\mathrm{HOMO}}$ the HOMO energy.

Incorporation of these conclusions yields the following expressions for the Fukui functions:

$$f_N^+(\bar{r}) = \left(\frac{\delta\, \varepsilon_{\mathrm{LUMO}}}{\delta\, v(\bar{r})}\right)_N \tag{12}$$

$$f_N^-(\bar{r}) = \left(\frac{\delta\, \varepsilon_{\mathrm{HOMO}}}{\delta\, v(\bar{r})}\right)_N \tag{13}$$

These new formulas are exact only for LDA- and GGA-type functionals.

Extending this for the dual descriptor, one finds that

$$f^{(2)}(\bar{r}) = 2\left(\frac{\delta \eta}{\delta\, v(\bar{r})}\right) \cong \left(\frac{\delta(\mu^+ - \mu^-)}{\delta\, v(\bar{r})}\right)_N = \left\{\frac{\delta(\varepsilon_{\mathrm{LUMO}} - \varepsilon_{\mathrm{HOMO}})}{\delta\, v(\bar{r})}\right\}_N \tag{14}$$

with η being the hardness, defined as the second derivative of the energy to the number of electrons.

2.2. Theoretical Method. The functional derivatives were calculated using the scheme described in ref 32. This technique can be used for evaluating the functional derivative of any property Q with respect to the external potential:

$$\left(\frac{\delta\, Q[v(r)]}{\delta\, v(\bar{r})}\right)_N \tag{15}$$

When the definition of a functional derivative is used, the responses of $Q[v(\bar{r})]$ to P perturbations $\{w_i(\bar{r})\}_{i=1}^{P}$ in the external potential can be written as

$$Q[v + w_i] - Q[v] = \int \left(\frac{\delta\, Q[v]}{\delta\, v(\bar{r})}\right)_N w_i(\bar{r})\, \mathrm{d}\bar{r} \quad \text{with } i \in \{1,\ 2,\ \ldots,\ P\} \tag{16}$$

This equation is only valid in the linear response regime, that is, only for small perturbations.

Expansion of the functional derivative in a basis set

$$\left(\frac{\delta\, Q[v(\bar{r})]}{\delta\, v(\bar{r})}\right)_N = \sum_{j=1}^{K} q_j\, \beta_j(\bar{r}) \tag{17}$$

gives

$$Q[v + w_i] - Q[v] = \sum_{j=1}^{K} q_j \int w_i(\bar{r})\, \beta_j(\bar{r})\ \mathrm{d}\bar{r} \quad \text{with } i \in \{1,\ 2,\ \ldots, P\} \tag{18}$$

This set of simultaneous linear equations for the coefficients of expansion can be rewritten as

$$\mathbf{d} = \mathbf{B}\mathbf{q} \tag{19}$$

where **B** is a $K \times P$ matrix with elements $B_{ij} = \int w_i(\bar{r})\, \beta_j(\bar{r})\, \bar{\mathrm{d}}r$, **d** is a P-dimensional column matrix with elements $d_i = Q[v + w_i] - Q[v]$, and **q** is a K-dimensional column matrix with elements q_i.

Equation 19 can be solved once $P > K$ using a linear least-squares fitting. In practice, P needs to be much larger than K to ensure convergence. If desired, the normalization of the calculated functional derivative can be imposed by adding an extra equation to the set.

2.3. Implementation. The external potential is perturbed using point charges which are randomly distributed around the molecule. The response of the HOMO and LUMO energy determines the matrix **d**. **B** is analytically computed from the basis set and the point charges. Equation 19 is then solved for **q**. Finally, substitution of the resulting expansion coefficients into eq 17 yields the desired functional derivative. In the case of the calculation of the Fukui functions, Q should be taken as $\varepsilon_{\mathrm{LUMO}}$ or $\varepsilon_{\mathrm{HOMO}}$ (see eqs 12 and 13).

The calculation of the dual descriptor occurs in a similar way, though the responses of the hardness with respect to variations in the external potential are needed. Using the "finite difference" approximation for the explicit calculation of the hardness, one finds

$$f^{(2)}(\bar{r}) = 2\left(\frac{\delta\eta}{\delta\, v(\bar{r})}\right)_N \cong \left(\frac{\delta\,(\mu^+ - \mu^-)}{\delta\, v(\bar{r})}\right)_N \tag{20}$$

For LDA and GGA functionals, this is equivalent to

$$\begin{aligned} f^{(2)}(\bar{r}) &= \left\{\frac{\delta(\varepsilon_{\mathrm{LUMO}} - \varepsilon_{\mathrm{HOMO}})}{\delta\, v(\bar{r})}\right\}_N \\ &= \left\{\left[\frac{\delta\, \varepsilon_{\mathrm{LUMO}}}{\delta\, v(\bar{r})}\right]_N - \left[\frac{\delta\, \varepsilon_{\mathrm{HOMO}}}{\delta\, v(\bar{r})}\right]_N\right\} \\ &= f^+(\bar{r}) - f^-(\bar{r}) \end{aligned} \tag{21}$$

The proposed calculation scheme for $f^{(2)}(\bar{r})$ is thus equal to the one in eq 6, except that the used Fukui functions are obtained using our alternative method.

3. Computational Details

All molecular structures were optimized at the B3LYP/6-311+G(d,f)[39] level of theory. Calculations of the energy and orbital energies were carried out using the Perdew−Becke−Enrzerhof (PBE) exchange-correlation functional and the 6-311++G(d) basis set.

All calculations were performed with Gaussian 03[40] in combination with the program described in refs 32 and 33. Contour plots were generated using Mathematica,[41] while isosurfaces are constructed with Gaussview.[42]

4. Results and Discussion

In the following section, we examine the reactivity of different molecules using local Fukui functions and the local dual descriptor computed with the perturbational method described above. We will first test its implementation, concentrating on local reactivity indices for the molecules CH_2O, SCN^-, and CO. Having established the reliability of the method, an elaborate set of more complex molecules will be investigated, focusing mainly on the results for the local dual descriptor.

4.1. Determination of Computational Parameters. An important issue when using the aforementioned perturbational technique for the calculation of Fukui functions is the determination of the optimal working parameters of the program, like the distribution, the size and the number of the point charges, and the option to enforce the normalization of the functions.

Prior to the determination of these parameters, we had to decide which basis set to use for the expansion of the functional derivatives, compare eq 17. In order to get an optimal accuracy, this basis set should be as flexible as possible and should also incorporate the decay of the density and its derivatives, which is twice as fast as the one for wave functions. These arguments lead to the choice of the Ahlrichs Coulomb Fitting auxiliary basis set,[43,44] which is a density-based basis set, typically used for the accelerated calculation of Coulomb integrals in DFT calculations.

For our purposes, the incorporation of only s and p functions is sufficient. The contraction coefficients are neglected, which makes the set more flexible.

The first parameter to be considered is the positioning of the point charges. Each of the point charges is randomly distributed around an atom in a volume defined by two concentric spheres with radii R_{min} and R_{max}, which are expressed in units of the van der Waals radius of the atom under consideration. As the functional derivative can only be accurate in regions where sampling has occurred, a large sampling region is required for the local calculation of functional derivatives. Consequently, we chose to place the point charges between 0.01 and 2.0 units of van der Waals radii of the composing atoms. This region, for example, corresponds to a sampling between distances of 0.02 and 4.43 Å from the nucleus for the hydrogen atom.

The magnitude of the point charges determines the size of the change of the orbital energies. Because we are restricted to the linear response region for the change in orbital energy, the determination of this parameter follows from a careful consideration between producing significant changes and remaining in the linear response region.

A comparison of a series of plots for the formaldehyde molecule for different acceptable point charge sizes showed

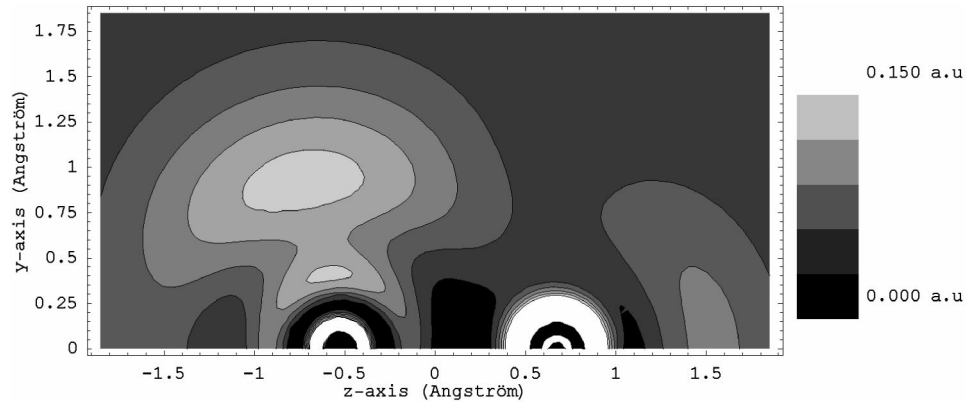

Figure 1. *f*(+) contourplot of the carbonyl group in formaldehyde in the plane perpendicular to the molecular plane. Coordinates: C at −0.52 Å, O at 0.67 Å on the *z* axis.

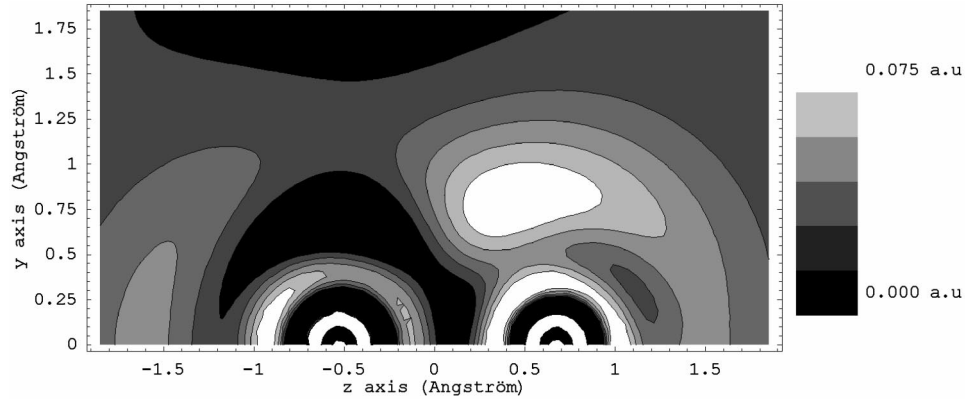

Figure 2. *f*(−) contourplot of the carbonyl group in formaldehyde in the plane perpendicular to the molecular plane. Coordinates: C at −0.52 Å, O at 0.67 Å on the *z* axis.

that the most reliable results were generated with point charges of 0.005 *e* or 0.010 *e*. Because of this, we chose to use fixed point charges of 0.005 *e*, which are automatically doubled if the orbital energy response is too small to be significant.

Finally, the only remaining parameter to be determined is the number of point charges we use. Since each placed point charge implies a single-point energy calculation, it is necessary to balance between an acceptable CPU time and a reliable convergence of the least-squares fitting. On the basis of the inspection of the molecular symmetry in the $f^+(r)$ contour plots for the molecular plane of CH_2O (i.e., does the local function show the correct molecular symmetry), we decided to use 400 point charges per atom. With the chosen set of working parameters and by adding a normalization equation with a weight of 1, normalizations turn out to be good and usually only differ from the exact values by a factor of 10^{-2} or even 10^{-3}.

4.2. Fukui Function Calculations of Small Molecules. Before turning to the dual descriptor, we will perform an analysis of CH_2O, SCN^-, and CO using Fukui functions with contour and isosurface plots, computed as described above.

Formaldehyde is a typical reference molecule for testing Fukui functions because of its reactive carbonyl group: the carbon atom is known to undergo nucleophilic attack, while the oxygen atom is the preferred site for an electrophilic attack. When this is taken into account, $f^+(\bar{r})$ should have large values around the carbon atom, while $f^-(\bar{r})$ should be large close to the oxygen atom. Figures 1 and 2, obtained with the perturbational method, depict contour plots of these functions for the carbonyl group in the plane perpendicular to the molecular plane.

As can be seen, the contour plots are marked by high Fukui function values in the neighborhood of the carbon atom for $f^+(\bar{r})$ and high $f^-(\bar{r})$ values for the oxygen atom, in perfect agreement with experimental reactivity and finite difference results.[24] Both plots reveal spurious fluctuations of the Fukui functions near the nucleus. This effect is a consequence of the limited sampling in the direct surroundings of the nuclei. Elaborate sampling in this region solves the problem but requires a significant increase of CPU time without generating any reactivity-related information.

Passing to carbon monoxide (CO), as an alternative to contour plots, isosurfaces are used. In view of the extensiveness of the isosurface in the direct environment of the carbon atom, this atom is predicted to be the most reactive for nucleophilic and electrophilic attacks. Nonetheless, both surfaces in Figure 3 have a distinct shape, indicating that the orientation of an incoming nucleophile or electrophile at the initial stage of the reaction might be different.

As a third case, we investigated the reactivity of the ambident nucleophile SCN^-, which possesses two reactive sites for an electrophilic attack.[45] In this situation, the hardness of the reactive site plays—via the HSAB principle—an important role in the selectivity.

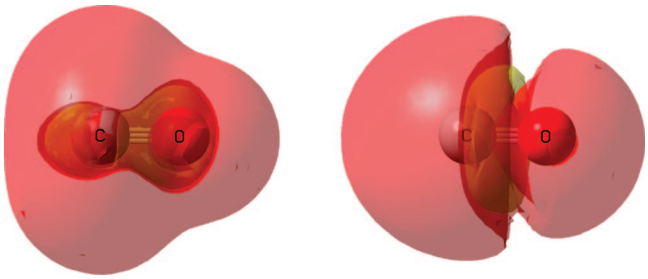

Figure 3. Isosurface (0.01 au) of *f*(+) and *f*(−) for CO.

It is well-known that, for anions, GGA functionals yield positive or very small HOMO energies, which exhibit considerable basis set dependence.[46] For that reason, μ^- was estimated using vertical ionization energies (eq 22), implying an extra single-point calculation of the $N - 1$ system for each perturbation.

$$\mu^- = \left(\frac{\partial E}{\partial N}\right)^-_{v(\bar{r})} = E_N - E_{N-1} \tag{22}$$

In Figure 4, we show the contourplot of $f^-(\bar{r})$ for the molecular plane of SCN^-. The results seem similar to the ones obtained in ref 47: the Fukui function clearly demonstrates that the softest reaction site is the sulfur atom. Hard electrophiles will prefer to interact with the nitrogen atom. These results are in agreement with experimental data,[45] as are the ones for two other typical ambident nucleophiles, CH_2CHO^- and NO_2^-, for which data can be found in the Supporting Information.

4.3. Application of Dual Descriptor to Small Molecules. The excellent quality of the Fukui functions using the perturbational approach gives the necessary confidence for the application of the new methodology in the computation of local descriptors. Hence, the local dual descriptor will be calculated for the molecules CH_2O and CO. The ambident nucleophile, SCN^-, will be left out of consideration, because its reactivity is almost entirely determined by describing its behavior toward electrophilic attacks, which is best characterized by f^- (cf. previous section).

Results of $f^{(2)}$ for formaldehyde are displayed in Figure 5: areas with $f^{(2)}(\bar{r}) > 0$ are susceptible to undergoing a nucleophilic attack, and areas with $f^{(2)}(\bar{r}) < 0$ are more likely to accept an electrophilic attack. As the Fukui functions (Figures 1 and 2), $f^{(2)}(\bar{r})$ generates the correct reactivity for the carbonyl of formaldehyde with positive values near the carbon atom and negative values close to the oxygen atom.

An interesting advantage of the dual descriptor is its ability to smoothen both Fukui functions involved. This effect also diminishes the spurious oscillations around the nuclear positions.

For CO, $f^{(2)}(\bar{r})$ sketches an image analogous to the Fukui functions (Figure 3), as the negative values of the descriptor (electrophilic attack) are mainly situated at the carbon terminus of the CO bond and positive values (nucleophilic attack) are located near the carbon atom in a tire-shaped way, positioned perpendicular to the bonding axis.

The preceding results can be seen as a generalization of the classical explanation for the bonding patterns observed in transition-metal−carbonyl compounds. In these systems, an interaction occurs between the (electrophilic) metal ion and the electrons in the CO HOMO orbital, which is mainly localized on the carbon atom, resulting in a bonding σ orbital. Further stabilization is then obtained through a π interaction between the electrons in the d orbitals of the metal (the nucleophile) and the LUMO of CO.[48]

4.4. Regioselectivity in Electrophilic Aromatic Substitution. Because of the remarkable selectivity difference between ortho/para and meta directors in electrophilic aromatic substitution (EAS) reactions,[49] which has already been studied in previous conceptual DFT work,[50,51] this reaction provides interesting test cases for the new perturbational method.

Since $f^{(2)}(\bar{r})$ is a combination of the Fukui functions for electrophilic and nucleophilic attack, it should give enough relevant information to elucidate the reactivity. In order to facilitate the interpretation of the ring reactivity, no fitting basis functions were placed on the hydrogen atoms.

First, phenol and aniline were considered. Their OH and NH_2 groups are electron donors that promote substitutions on ortho and para positions in an EAS.

Figure 7 depicts the results for $f^{(2)}(\bar{r})$; the yellow regions correspond to zones with a negative dual descriptor which are susceptible to an electrophilic attack. These regions are the most pronounced for the para positions, whereas the reactivity of the ortho positions, which are expected to be susceptible to undergoing electrophilic attacks too, is less clear. Therefore, the same isosurfaces are shown from another angle in Figure 8. In these figures, one can see small nested zones at the ortho positions which are sensible for an electrophilic attack.

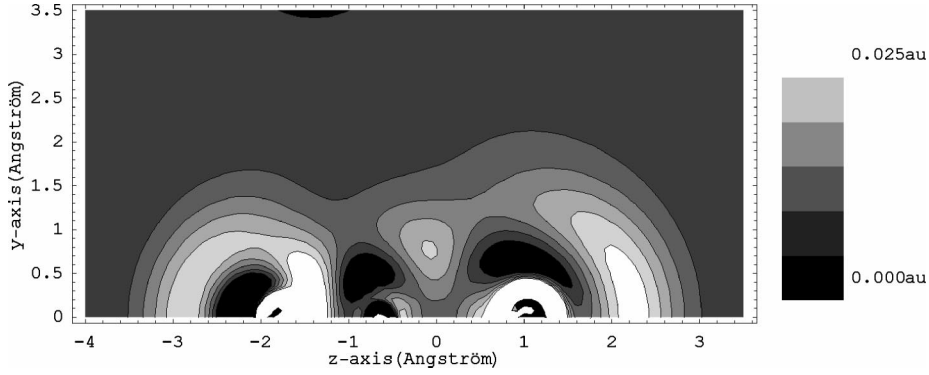

Figure 4. *f*(−) contourplot of SCN^-. Coordinates of the atoms in Å: N at −1.81, C at −0.63, and S at 1.03 on the *z*-axis.

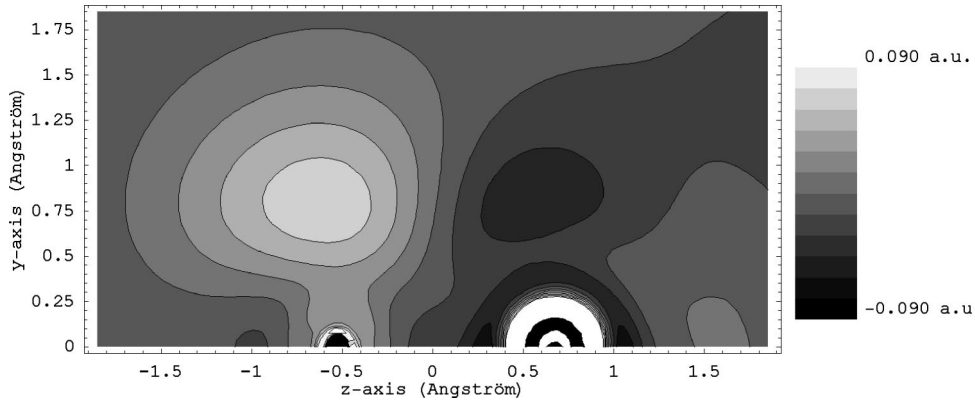

Figure 5. $f^{(2)}$ contourplot of the carbonyl group in formaldehyde in the plane perpendicular to the molecular plane. Coordinates: C at −0.52 Å, O at 0.67 Å on the *z* axis.

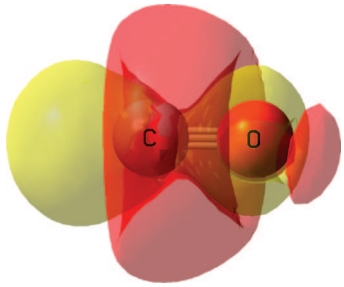

Figure 6. Isosurface of $f^{(2)}$ (0.02 au, positive regions are red, negative regions are yellow) for CO.

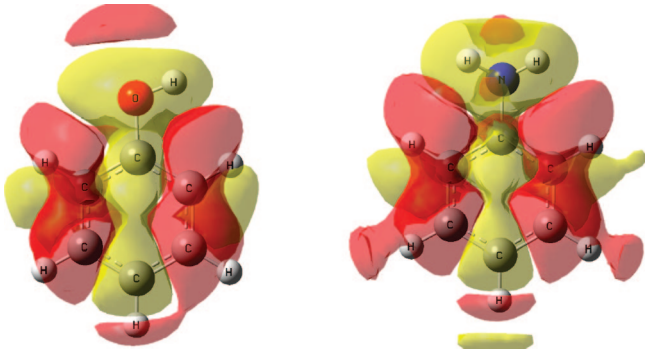

Figure 7. View of the isosurface of $f^{(2)}$ (0.002 au, positive regions are red, negative regions are yellow) for the molecular plane of phenol and aniline.

Next, two deactivating, meta-directing cases, benzaldehyde and cyanobenzene, were calculated.

As can be seen in Figure 9, an important reactivity switch occurred in comparison with the ortho/para directors. For cyanobenzene, the para position is clearly deactivated for an electrophilic attack, while the meta position now exhibits a yellow region. Quite surprisingly, the bond between the ipso and ortho positions is surrounded by a yellow surface. An inspection of the finite difference $f^{(2)}(\bar{r})$ at the same level of theory (PBE/6-311++G(d,f)) reveals good agreement with the results of the perturbational method. Deviations of our results from the previously obtained finite difference results[27] at the Hartree−Fock (HF/6-311G(d,f)) level, which do not predict an ipso reactivity, could thus be ascribed to the use of the PBE functional in the DFT calculations.[52,53]

Results for benzaldehyde pose another difficulty because no specific reactivity pattern can be recognized in the

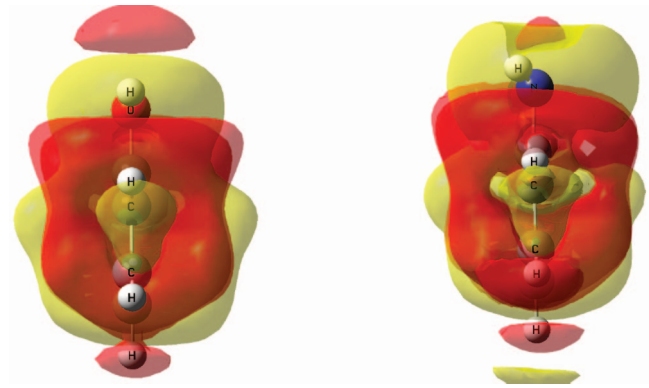

Figure 8. View of the isosurface of $f^{(2)}$ (0.002 au, positive regions are red, negative regions are yellow) for the plane perpendicular to the molecular plane of phenol and aniline.

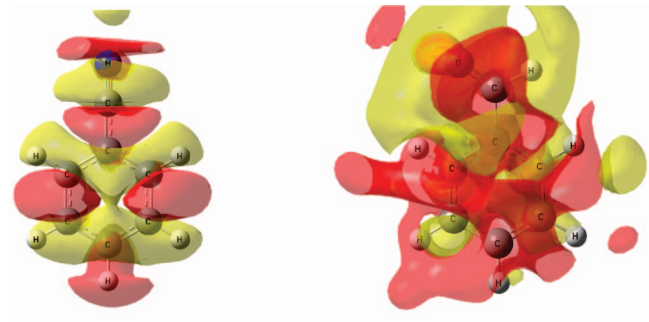

Figure 9. View of the isosurface of $f^{(2)}$ (0.002 au, positive red, negative yellow) for the molecular plane of cyanobenzene and benzaldehyde.

isosurface of Figure 9, whereas the finite difference dual descriptor (PBE/6-311++G(d)) is able to predict a more realistic reactivity. In search of possible explanations, the composing Fukui functions were examined. Primarily, $f^{-}(\bar{r})$ exhibited strange behavior with a reactivity concentrated on the substituent, leaving the ring basically inactive for an EAS. As previously explained, $f^{-}(\bar{r})$ is constructed from the responses of the HOMO energy. A plot of the HOMO density reveals that this orbital is predominantly located on the substituent and is thus unable to predict the correct ring reactivity. Since the two lower-lying orbitals are located on the aromatic ring, we used these orbitals together with the HOMO in order to obtain an adjusted version of $f^{-}(\bar{r})$:

$$f^{-}(\bar{r}) = \left(\frac{\delta\,(\varepsilon_{\mathrm{HOMO}} + \varepsilon_{\mathrm{HOMO-1}} + \varepsilon_{\mathrm{HOMO-2}})/3}{\delta\, v(\bar{r})} \right)_N \quad (23)$$

Figure 10 shows that the adjusted $f^{-}(\bar{r})$ (eq 23) improves the reactivity picture. Meta positions exhibit yellow regions; nonetheless, the rest of the ring, mainly the ortho−ipso bond, presents similar behavior. The improved results obtained with formula 23 suggest the occurrence of orbital mixing during the different perturbations: when several orbitals are close in energy, different perturbations will access different orbitals.[54–56] Because the inclusion of the three highest orbitals does not provide a perfect prediction of the chemical reactivity yet, it may be necessary to include additional orbitals in eq 23. It is also possible that the present method—which models an infinitesimal change in the number of electrons—does not adequately predict the orbital relaxation contribution to the Fukui function.[50,57–60] (It is known, for example, that DFT functionals are more accurate for an integer electron number than they are for a fractional electron number.[61]) So, it is also possible that a more-accurate model of orbital relaxation effects would bring the picture in Figure 10 into closer agreement with the experimentally observed reactivity preferences.

In addition, the Supporting Information contains a number of other molecules like propene, propenal, ethanal, propanon, and chlorobenzene that were tested with the perturbational method. In all of the cases, the dominant reactivity for electrophilic addition, nucleophilic addition, and electrophilic aromatic substitution was recovered with regard to experimental results.

5. Conclusions

We have given a validation of and extension to the perturbational method[32,33] for the calculation of DFT-based reactivity descriptors by computing local Fukui functions and the dual descriptor. The method is based on a Maxwell relation to circumvent the need to take the derivatives with respect to the number of electrons and uses functional derivatives with respect to the external potential instead.

The results confirm the usefulness of the dual descriptor as a new reactivity index for electrophilic and nucleophilic attacks. Moreover, the convincing results for both the Fukui functions ($(\delta\mu/\delta v(\bar{r}))_N$) and the dual descriptor ($(\delta\eta/\delta v(\bar{r}))_N$) also indicate the general validity of the perturbational approach, making it an interesting methodology for the calculation of functional derivatives to the external potential of any global property.

As such, the long-lasting problem concerning DFT-based reactivity descriptors involving derivatives with respect to the number of electrons can successfully be circumvented by switching to expressions with functional derivatives to the external potential, obtained using Maxwell relations.

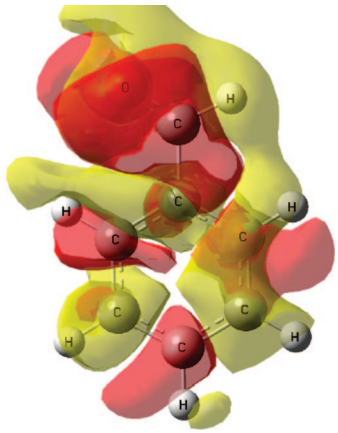

Figure 10. View of isosurface of $f^{(2)}$ (0.002 au, positive regions are red, negative regions are yellow) for the molecular plane of benzaldehyde using adjusted formula 23.

Acknowledgment. T.F. and N.S. thank the Fund for Scientific Research Flanders (FWO) for a predoctoral (Aspirant) fellowship. P.G and F.D.F thank the Fund for Scientific Research Flanders (FWO) and the VUB for their continuous support. P.W.A. would like to thank NSERC, the Canada Research Chairs, and SHARCNET for research support.

Supporting Information Available: A PDF file containing contourplots of $f^{-}(\bar{r})$ for ambident nucleophiles NO_2^- and CH_2CHO^- and isosurfaces of $f^{(2)}(\bar{r})$ for propene, propanon, ethanal, and chlorobenzene is included. This information is available free of charge via the Internet at http://pubs.acs.org.

References

(1) Hohenberg, P.; Kohn, W. *Phys. Rev. B: Condens. Matter Mater. Phys.* **1964**, *136*, 864–871.

(2) Kohn, W.; Sham, L. J. *Phys. Rev. A: At., Mol., Opt. Phys.* **1965**, *140*, 1133–1138.

(3) Kohn, W.; Becke, A. D.; Parr, R. G. *J. Phys. Chem.* **1996**, *100*, 12974–12980.

(4) Kohn, W. *Rev. Mod. Phys.* **1999**, *71*, 1253–1266.

(5) Becke, A. D. *J. Chem. Phys.* **1993**, *98*, 5648–5652.

(6) Perdew, J. P.; Ruzsinszky, A.; Tao, J.; Staroverov, V. N.; Scuseria, G. E.; Csonka, G. I. *J. Chem. Phys.* **2005**, *123*, 062201.

(7) Chermette, H. *J. Comput. Chem.* **1999**, *20*, 129–154.

(8) Geerlings, P.; De Proft, F.; Langenaeker, W. *Chem. Rev.* **2003**, *103*, 1793–1874.

(9) Parr, R. G.; Yang, W. *Density Functional Theory of Atoms and Molecules*; Oxford University Press: New York, 1989; p 333.

(10) Ayers, P. W.; Anderson, J. S. M.; Bartolotti, L. J. *Int. J. Quantum Chem.* **2005**, *101*, 520–534.

(11) Parr, R. G.; Donnelly, R. A.; Levy, M.; Palke, W. E. *J. Chem. Phys.* **1978**, *68*, 3801–3807.

(12) Parr, R. G.; Pearson, R. G. *J. Am. Chem. Soc.* **1983**, *105*, 7512–7516.

(13) Yang, W.; Parr, R. G. *Proc. Natl. Acad. Sci. U.S.A.* **1985**, *82*, 6723–6726.

(14) Nalewajski, R. F.; Parr, R. G. *J. Chem. Phys.* **1982**, *77*, 399–407.

(15) Parr, R. G.; Yang, W. *J. Am. Chem. Soc.* **1984**, *106*, 4049–4050.

(16) Perdew, J. P.; Parr, R. G.; Levy, M.; Balduz, J. L. *Phys. Rev. Lett.* **1982**, *49*, 1691–1694.

(17) Zhang, Y.; Yang, W. *Theor. Chem. Acc.* **2000**, *103*, 346–348.

(18) Yang, W.; Zhang, Y.; Ayers, P. W. *Phys. Rev. Lett.* **2000**, *4*, 5172–5175.

(19) Ayers, P. W.; Levy, M. *Theor. Chem. Acc.* **2000**, *103*, 353–360.

(20) Ayers, P. W.; Parr, R. G. *J. Am. Chem. Soc.* **2000**, *122*, 2010–2018.

(21) Ayers, P. W. *J. Math. Chem.* **2008**, *43*, 285–303.

(22) Mori-Sanchez, P.; Cohen, A. J.; Yang, W. T. *J. Chem. Phys.* **2006**, *125*, 201102.

(23) Michalak, A.; De Proft, F.; Geerlings, P.; Nalewajski, R. F. *J. Phys. Chem. A* **1999**, *103*, 762–771.

(24) Geerlings, P.; De Proft, F.; Langenaeker, W. *Chem. Rev.* **2003**, *103*, 1808.

(25) Tozer, D. J.; Handy, C. H. *Mol. Phys.* **2003**, *101*, 2669–2675.

(26) Geerlings, P.; De Proft, F. *Phys. Chem. Chem. Phys.* **2008**, *10*, 3028–3042.

(27) Morell, C.; Grand, A.; Toro-Labbé, A. *J. Phys. Chem. A* **2005**, *109*, 205–212.

(28) Morell, C.; Grand, A.; Toro-Labbé, A. *Chem. Phys. Lett.* **2006**, *425*, 342–346.

(29) Morale, C. Un nouveau descripteur de la reactivité locale, Ph.D. Thesis, Université de Grenoble, Grenoble, France, 2006; p 133.

(30) Morell, C.; Grand, A.; Gutiérrez-Oliva, S.; Toro-Labbé, A. Using the reactivity-selectivity descriptor $\Delta f(\bar{r})$ in organic chemistry. In *Theoretical Aspects of Chemical Reactivity*; Toro-Labbé, A., Ed.; Elsevier: Amsterdam, The Netherlands, 2006; pp 101−118.

(31) Ayers, P. W.; Morell, C.; De Proft, F.; Geerlings, P. *Chem.—Eur. J.* **2007**, *13*, 8240–8247.

(32) Ayers, P. W.; De Proft, F.; Borgoo, A.; Geerlings, P. *J. Chem. Phys.* **2007**, *126*, 224107.

(33) Sablon, N.; Ayers, P. W.; De Proft, F.; Geerlings, P. *J. Chem. Phys.* **2007**, *126*, 224108.

(34) Perdew, J. P.; Burke, M.; Ernzerhof, M. *Phys. Rev. Lett.* **1996**, *77*, 3865–3868.

(35) Perdew, J. P.; Burke, M.; Ernzerhof, M. *Phys. Rev. Lett.* **1997**, *78*, 1396–1396.

(36) Perdew, J. P.; Levy, M. *Phys. Rev. Lett.* **1983**, *51*, 1884–1887.

(37) Sham, L. J.; Schluter, M. *Phys. Rev. Lett.* **1983**, *51*, 1888–1891.

(38) Perdew, J. P.; Levy, M. *Phys. Rev. B: Condens. Matter Mater. Phys.* **1997**, *56*, 16021–16028.

(39) Krishnan, R.; Frisch, M. J.; Pople, J. A. *J. Chem. Phys.* **1980**, *72*, 4244–4245.

(40) Frisch, M. J. ; Trucks, G. W.; Schlegel, H. B.; Scuseria, G. E.; Robb, M. A.; Cheeseman, J. R.; Montgomery, J. A., Jr.; Vreven, T.; Kudin, K. N.; Burant, J. C.; Millam, J. M.; Iyengar, S. S.; Tomasi, J.; Barone, V.; Mennucci, B.; Cossi, M.; Scalmani, G.; Rega, N.; Petersson, G. A.; Nakatsuji, H.; Hada, M.; Ehara, M.; Toyota, K.; Fukuda, R.; Hasegawa, J.; Ishida, M.; Nakajima, T.; Honda, Y.; Kitao, O.; Nakai, H.; Klene, M.; Li, X.; Knox, J. E.; Hratchian, H. P.; Cross, J. B.; Bakken, V.; Adamo, C.; Jaramillo, J.; Gomperts, R.; Stratmann, R. E.; Yazyev, O.; Austin, A. J.; Cammi, R.; Pomelli, C.; Ochterski, J. W.; Ayala, P. Y.; Morokuma, K.; Voth, G. A.; Salvador, P.; Dannenberg, J. J.; Zakrzewski, V. G.; Dapprich, S.; Daniels, A. D.; Strain, M. C.; Farkas, O.; Malick, D. K.; Rabuck, A. D.; Raghavachari, K.; Foresman, J. B.; Ortiz, J. V.; Cui, Q.; Baboul, A. G.; Clifford, S.; Cioslowski, J.; Stefanov, B. B.; Liu, G.; Liashenko, A.; Piskorz, P.; Komaromi, I.; Martin, R. L.; Fox, D. J.; Keith, T.; Al-Laham, M. A.; Peng, C. Y.; Nanayakkara, A.; Challacombe, M.; Gill, P. M. W.; Johnson, B.; Chen, W.; Wong, M. W.; Gonzalez, C.; Pople, J. A. *Gaussian 03*, Revision D.01; Gaussian, Inc.: Wallingford, CT, 2004.

(41) *Mathematica*, Version 5.2; Wolfram Research, Inc.: Champaign, IL, 2005.

(42) *GaussView*, Version 3.09; Dennington, R., II, Keith, T., Millam, J., Eppinnett, K., Hovell, W. L., Gilliland, R., Eds.; Semichem, Inc.: Shawnee Mission, KS, 2003.

(43) Eichkorn, K.; Treutler, O.; Öhm, H.; Häser, M.; Ahlrichs, R. *Chem. Phys. Lett.* **1995**, *240*, 283–289.

(44) Eichkorn, K.; Weigend, F.; Treutler, O.; Ahlrichs, R. *Theor. Chem. Acc.* **1997**, *97*, 119–124.

(45) Hudson, R. F. Nucleophilic Reactivity. In *Chemical Reactivity and Reaction Paths*; Klopman, G., Ed.; Wiley: New York, 1974; pp 167−252.

(46) Simons, J.; Jordan, K. D. *Chem. Rev.* **1987**, *87*, 535–555.

(47) Langenaeker, W.; De Proft, F.; Geerlings, P. *THEOCHEM* **1996**, *362*, 175–179.

(48) Atkins, P.; Overton, T.; Rourke, J.; Weller, M.; Amstrong, F. *Inorganic Chemistry*, 4th ed.; Oxford University Press: Oxford, United Kingdom, 2006; pp. 59.

(49) Clayden, J.; Greeves, N.; Warren, S.; Wothers, P. *Organic Chemistry*; Oxford University Press: Oxford, United Kingdom, 2001; pp 547−579.

(50) Langenaeker, W.; De Proft, F.; Geerlings, P. *J. Phys. Chem.* **1995**, *99*, 6424–6431.

(51) De Proft, F.; Van Alsenoy, C.; Peeters, A.; Langenaeker, W.; Geerlings, P. *J. Comput. Chem.* **2002**, *23*, 1198–1209.

(52) Langenaeker, W.; Demel, K.; Geerlings, P. *THEOCHEM* **1991**, *80*, 329–342.

(53) Anderson, J. S. M.; Melin, J.; Ayers, P. W. *J. Chem. Theory Comput.* **2007**, *3*, 375–389.

(54) da Silva, R. R.; Ramalho, T. C.; Santos, J. M.; Figueroa-Villar, J. D. *J. Phys. Chem. A* **2006**, *110*, 1031–1040.

(55) Maksic, Z. B.; Vianello, R. *J. Phys. Chem. A* **2006**, *110*, 10651–10652.

(56) da Silva, R. R.; Ramalho, T. C.; Santos, J. M.; Figueroa-Villar, J. D. *J. Phys. Chem. A* **2006**, *110*, 10653–10654.

(57) Yang, W.; Parr, R. G.; Pucci, R. *J. Chem. Phys.* **1984**, *81*, 2862–2863.

(58) Bartolotti, L. J.; Ayers, P. W. *J. Phys. Chem. A* **2005**, *109*, 1146–1151.

(59) Ayers, P. W. *Phys. Chem. Chem. Phys.* **2006**, *8*, 3387–3390.

(60) Melin, J.; Ayers, P. W.; Ortiz, J. V. *J. Phys. Chem. A* **2007**, *111*, 10017–10019.

(61) Zhang, Y.; Yang, W. *J. Chem. Phys.* **1998**, *109*, 2604–2608.

CT800027E